

# Magnetron Sputtering of Antibacterial and Antifungal Tantalum-Copper and Niobium-Copper Coatings on Three Dimensional-Printed Porous Titanium Alloy Scaffolds: Part II

## Precise deposition of coatings

### Bagdat Azamatov<sup>§</sup>

Smart Engineering Competence Centre,  
D. Serikbayev East Kazakhstan Technical  
University, 19 Serikbayev Street, 070010  
Ust-Kamenogorsk, Kazakhstan

### Alexandr Borisov

Smart Engineering Competence Centre,  
D. Serikbayev East Kazakhstan Technical  
University, 19 Serikbayev Street, 070010  
Ust-Kamenogorsk, Kazakhstan

### Bauyrzhan Maratuly

Smart Engineering Competence Centre,  
D. Serikbayev East Kazakhstan Technical  
University, 19 Serikbayev Street, 070010  
Ust-Kamenogorsk, Kazakhstan

### Dmitry Dogadkin

Smart Engineering Competence Centre,  
D. Serikbayev East Kazakhstan Technical  
University, 19 Serikbayev Street, 070010  
Ust-Kamenogorsk, Kazakhstan

### Yuliya Safarova (Yantsen)<sup>‡</sup>

Laboratory of Bioengineering and Regenerative  
Medicine, National Laboratory Astana,  
Nazarbayev University, 010000 Astana,  
Kazakhstan

### Ridvan Yamanoglu<sup>¶</sup>

Department of Metallurgical and Materials  
Engineering, Faculty of Engineering, Kocaeli  
University, 41001, Kocaeli, Turkey

### Darya Alontseva<sup>\*</sup>

School of Digital Technologies and Artificial  
Intelligence, D. Serikbayev East Kazakhstan  
Technical University, 19 Serikbayev Street,  
070010 Ust-Kamenogorsk, Kazakhstan

Email: <sup>‡</sup>yantsen@nu.edu.kz; <sup>§</sup>bazamatov@ektu.kz;  
<sup>¶</sup>ryamanoglu@kocaeli.edu.tr; <sup>\*</sup>dalontseva@ektu.kz

## PEER REVIEWED

Received 21st February 2024; Revised 30th April  
2024; Accepted 14th May 2024; Online 15th May  
2024

This is Part II of a study on the antimicrobial efficacy of tantalum-copper and niobium-copper coatings, applied *via* magnetron sputtering (MS) on three dimensional (3D) printed porous Ti6Al4V alloy scaffolds and gas-abrasive treated Ti6Al4V alloy, against *Staphylococcus aureus* and *Candida albicans*. Thicker coatings were found to show superior antimicrobial activity; however, thin niobium-copper coatings and uncoated alloy did not exhibit inhibitory effects. The release dynamics of copper ions from tantalum-copper coatings into physiological solution, analysed over ten days *via* inductively coupled plasma mass spectrometry, matched the inhibition zone growth. These findings support the potential of these coatings in developing endoprosthesis implants with enhanced antimicrobial properties.

## Keywords

magnetron-sputtered coating, titanium endoprosthesis implants, additive manufacturing, bacterial resistance, selective laser melting

This paper follows Part I (1) of the present study.

## Results and Discussion

An SEM image of the surface of Ti6Al4V alloy substrate after gas abrasive treatment and the results of measuring its surface roughness are presented in **Figure 1**. The Sa was  $4.6 \pm 1 \mu\text{m}$ , which is in complete agreement with the literature data (2, 3). Grit-blasted specimens in this work have comparable roughness with results from Lewallen *et al.* ( $R_a 5.74 \pm 0.19 \mu\text{m}$ ) and higher than bead-blasted substrates ( $R_a 1.10 \pm 0.18 \mu\text{m}$ ) (2). The surface topography of biomedical titanium alloys significantly influences their mechanical and biological properties, as detailed in the existing literature (4). The 3D surface of the Ti6Al4V alloy after gas abrasive treatment exhibited randomly formed valleys and peaks with maximum heights around  $12.5 \pm 1 \mu\text{m}$  and  $13.5 \pm 1 \mu\text{m}$ , respectively. The microtopographical complexity and micron-scale roughness of these surface features can create favourable sites for protein adsorption and improve the long-term stability of implants. Additionally, they also contribute significantly to the antibacterial activity of metallic biomaterials (4).

The results of measuring the thickness of MS coatings on Ti6Al4V alloy substrates subjected to gas abrasive treatment are presented in **Figures 2** and **3**, respectively.

As shown in **Figure 2(a)** and **Figure 3(a)**, the average thickness of niobium-copper and

tantalum-copper coatings of Group 1 (Table II in Part I of this review (1)), was  $2.24 \pm 0.8 \mu\text{m}$ . At the same time, the average thickness of niobium-copper and tantalum-copper coatings of Group 2 (Table II in Part I of this review (1)), was  $10.73 \pm 2.8 \mu\text{m}$  (**Figure 2(b)** and **Figure 3(b)**). From **Figures 2** and **3**, it can also be concluded that direct current magnetron sputtering (DC-MS) makes it possible to obtain coatings of the same thickness on the rough surface of a titanium alloy after gas abrasive treatment.

SEM images of MS tantalum-copper coatings on 3D-printed porous scaffolds are shown in **Figure 4**. As seen in **Figure 4**, MS allows for a uniform coating on the porous and rough surface of the scaffold, leaving the pores open, which is vital for the future ingrowth of the implant into the bone.

A closer examination of the microstructure of the MC coating on a porous scaffold (**Figure 5**) shows that the coating is formed by spherical particles, presumably a tantalum-copper alloy since the shade of grey in the SEM image of these particles is uniform, that is, there are no individual copper particles and tantalum particles. As can be seen from **Figure 5**, these particles partially melted completely and coated the substrate with a smooth layer (**Figure 5(a)**), but partially have a spherical shape with a rough surface (**Figure 5(b)**). As the particle sizes and their chemical composition are determined by the MS parameters, mainly the DC current on the target and the sputtering distance; further research is required to establish the relationship between the MS parameters and the composition of the dual coating, as well as the morphology of its surface.

The results of EDX analysis, illustratively presented in **Figure 6** and **Table I** for the niobium-copper coating, as well as in **Figure 7** and **Table II**

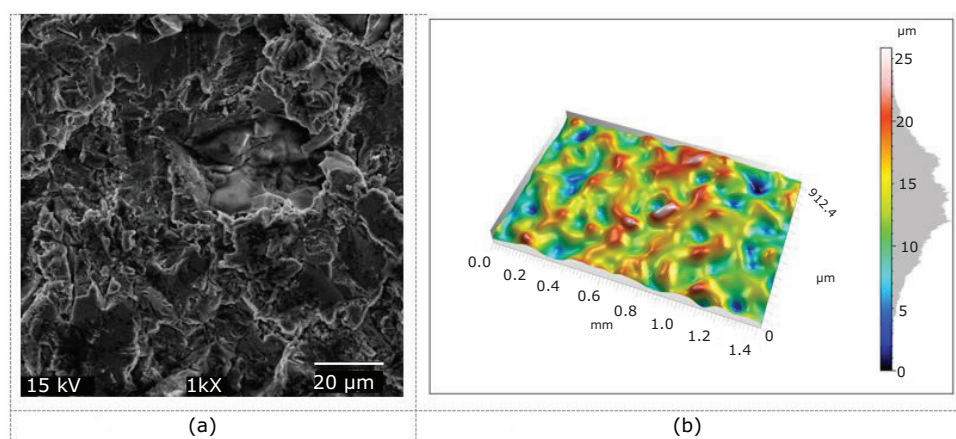


Fig. 1. Ti6Al4V alloy after gas abrasive treatment: (a) SEM image; (b) 3D surface topography

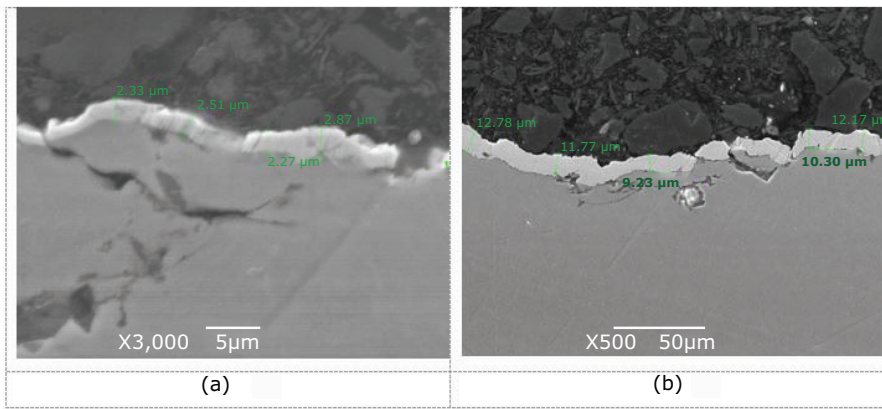


Fig. 2. SEM images of Ti6Al4V alloy after gas-abrasive treatment coated with MS niobium-copper coating: (a) Group 1; (b) Group 2

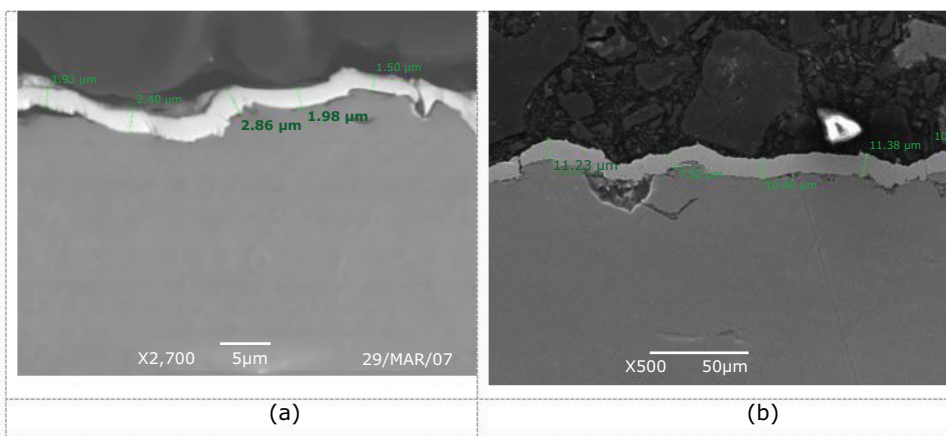


Fig. 3. SEM images of Ti6Al4V alloy after gas-abrasive treatment coated with MS tantalum-copper coating: (a) Group 1; (b) Group 2

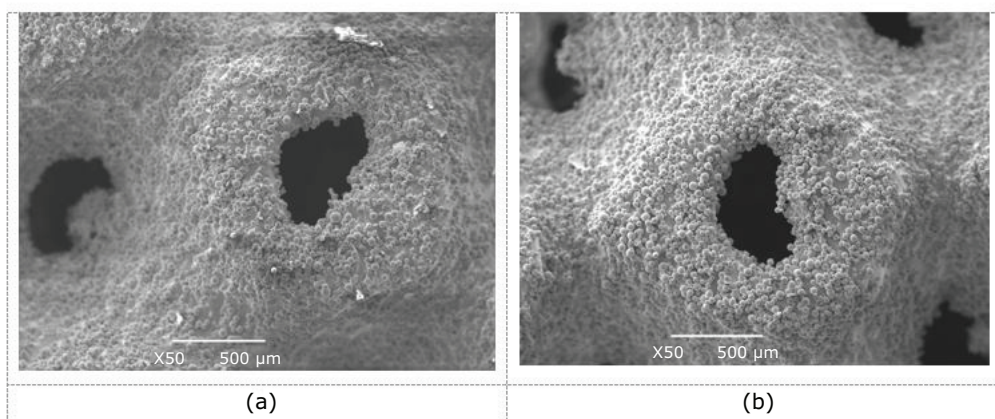


Fig. 4. SEM images of MS tantalum-copper coatings on 3D printed porous scaffolds: (a) the coating from Group 1; (b) the coating from Group 2

for the tantalum-copper coating, show that the desired component ratios of 75%Nb-25%Cu and 75%Ta-25%Cu were generally achieved.

Based on the results of statistical processing of EDX analysis data of five spectra for five specimens of each coating (Table II in Part I of this review (1)), it was established that for thin

(Group 1) and thick (Group 2) coatings of the copper-tantalum composition, an approximate ratio of 75% Ta-25%Cu is maintained with an average measurement error of 1.05 wt%, while for both groups of coatings of the copper-niobium composition the element ratio is approximately 75%Nb-25%Cu with an average measurement

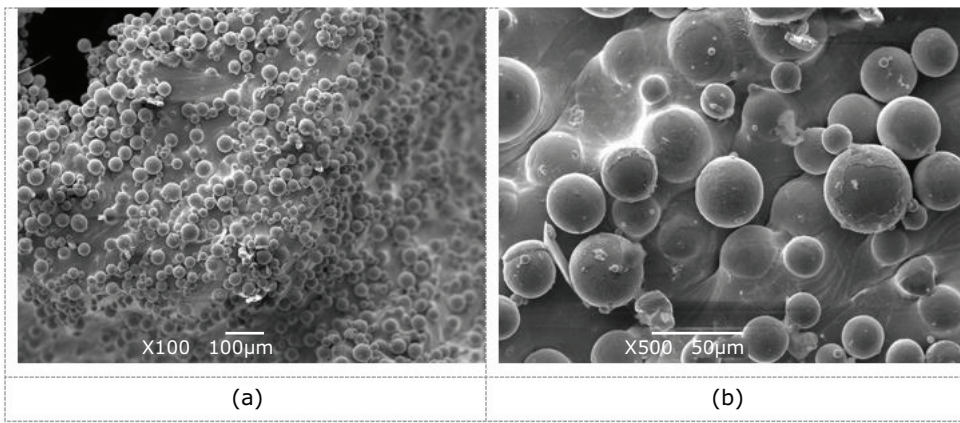


Fig. 5. SEM images of the MS tantalum-copper coating from Group 1 on 3D printed porous scaffold: (a) the area near the scaffold pore with partially melted coating particles; (b) un-melted coating particles

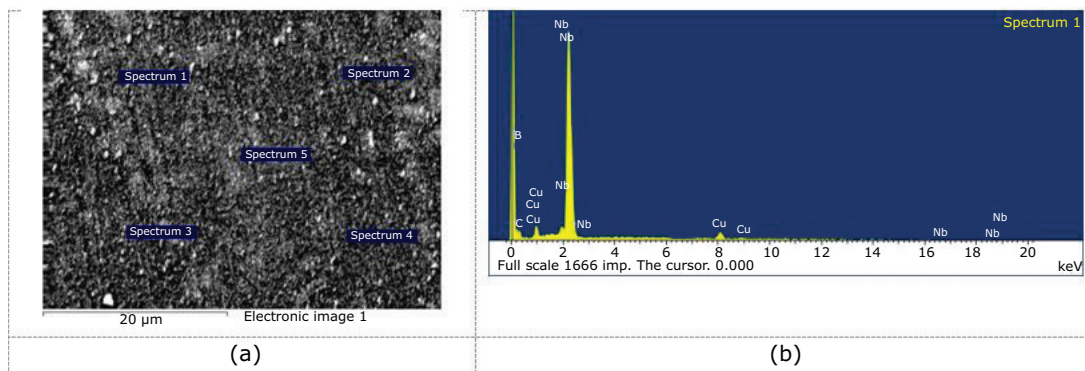


Fig. 6. (a) SEM image of the niobium-copper coating surface indicating areas of EDX analysis, that is, the location of the spectra; (b) the results of spectrum analysis

**Table I Data (in wt%) of the Normalised Results of EDX Analysis of all Elements in the Spectra of the Niobium-Copper Coating Shown in Figure 6(a)**

| Spectrum           | In stats | Cu    | Nb    | Total  |
|--------------------|----------|-------|-------|--------|
| Spectrum 1         | Yes      | 24.18 | 75.82 | 100.00 |
| Spectrum 2         | Yes      | 24.41 | 75.59 | 100.00 |
| Spectrum 3         | Yes      | 24.56 | 75.44 | 100.00 |
| Spectrum 4         | Yes      | 23.67 | 76.33 | 100.00 |
| Spectrum 5         | Yes      | 25.43 | 74.57 | 100.00 |
| Mean               | n/a      | 24.45 | 75.55 | 100.00 |
| Standard deviation | n/a      | 0.64  | 0.64  | -      |
| Max.               | n/a      | 25.43 | 76.33 | -      |
| Min.               | n/a      | 23.67 | 74.57 | -      |

Processing option: All elements analysed (normalised). All results in wt%

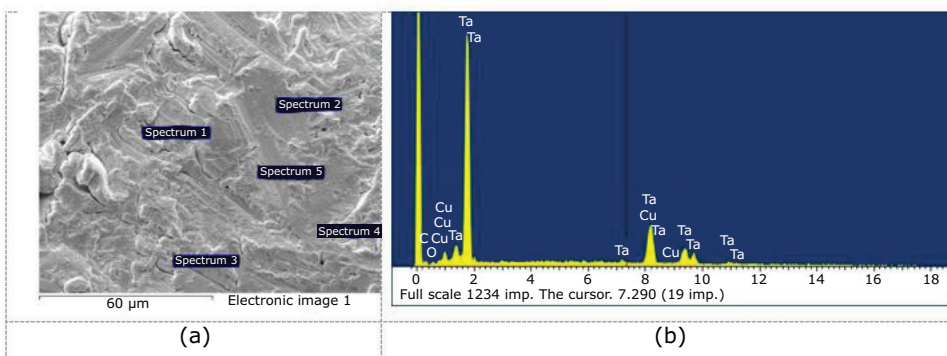


Fig. 7. (a) SEM image of the tantalum-copper coating surface indicating areas of EDX analysis, that is, the location of the spectra; (b) the results of spectrum analysis

error of 0.85 wt%. It is a rough estimate of the coating composition, chosen for a pilot experiment due to the convenience and clarity of the method to ensure that the MS parameters provide a coating composition close to the specification; in the future, a more accurate full spectral analysis of the coating composition will be carried out. Future research will focus on optimising parameters and conditions for DC-MS to achieve coatings with uniform thickness and precisely controlled composition.

*In vitro* experiments with agar well diffusion technique showed that the thicker coatings of tantalum-copper and niobium-copper from Group 2 were effective in suppressing *Staphylococcus aureus* proliferation, with the zones of inhibition ranging between 17.0–24.0 mm for tantalum-copper and

14.5–25.0 mm for niobium-copper (Figure 8). On the other hand, the thinner tantalum-copper coatings from Group 1 also presented a notable antimicrobial effect, hindering bacterial growth up to a zone of 20.0 mm. However, the thinner niobium-copper coatings from Group 1 did not demonstrate any significant bactericidal activity (Figure 8).

Similarly, in testing against the *Candida albicans* strain (Figure 9), thin tantalum-copper coatings (Group 1) created a growth delay zone of up to 12.0 mm; thicker tantalum-copper coatings (Group 2) generated inhibition zones ranging from 13.0 mm to 17.0 mm; and thick niobium-copper coatings (Group 2) produced a delay zone of up to 15.5 mm. However, thin niobium-copper coatings

**Table II Data (in wt%) of the Normalised Results of EDX Analysis of all Elements in the Spectra of the Tantalum-Copper Coating Shown in Figure 6(a)**

| Spectrum           | In stats | Cu    | Ta    | Total  |
|--------------------|----------|-------|-------|--------|
| Spectrum 1         | Yes      | 23.91 | 76.09 | 100.00 |
| Spectrum 2         | Yes      | 24.01 | 75.99 | 100.00 |
| Spectrum 3         | Yes      | 23.28 | 76.72 | 100.00 |
| Spectrum 4         | Yes      | 24.08 | 75.92 | 100.00 |
| Spectrum 5         | Yes      | 24.43 | 75.57 | 100.00 |
| Mean               | n/a      | 23.94 | 76.05 | 100.00 |
| Standard deviation | n/a      | 0.41  | 0.41  | -      |
| Max.               | n/a      | 24.43 | 76.72 | -      |
| Min.               | n/a      | 23.28 | 75.57 | -      |

Processing option: All elements analysed (normalised). All results in wt%

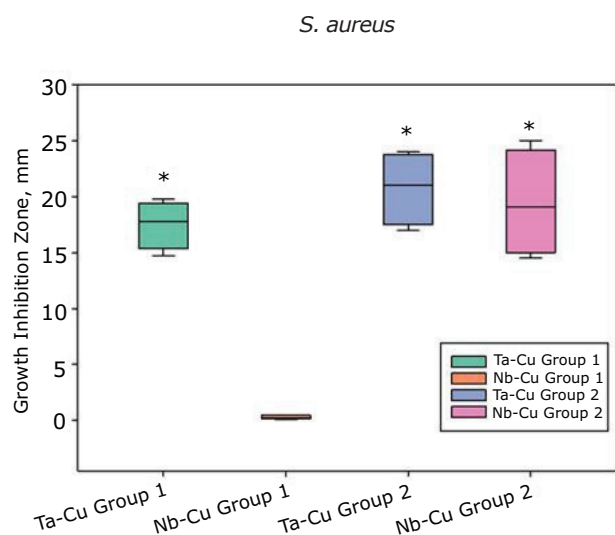


Fig. 8. Evaluation of inhibitory zones for various coatings against *S. aureus* growth (\* = p value ≤ 0.05 compared to the niobium-copper Group 1)

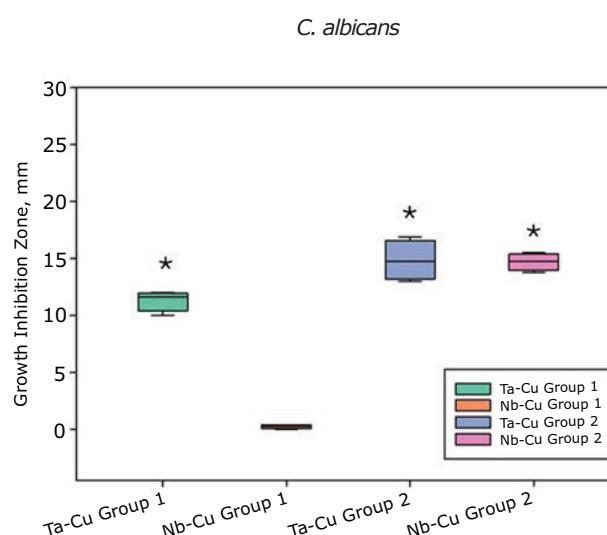


Fig. 9. Evaluation of inhibitory zones for various coatings against *C. albicans* growth (\* = p value ≤ 0.05 compared to the niobium-copper Group 1)

(Group 1) did not show antifungal activity. The Ti6Al4V titanium alloy after gas-abrasive treatment did not influence the growth and development of the bacteria and fungi studied within the given timeframe. The results are the average of four independent measurement series, with a relative measurement error not exceeding 3%.

Consequently, the thicker tantalum-copper coatings (Group 2) displayed the most significant antifungal properties and, along with the thick niobium-copper coatings, also demonstrated the highest antibacterial properties.

In tests conducted against *Candida albicans*, the thinner tantalum-copper coatings (Group 1) exhibited a notable antifungal effect, creating a zone of delayed growth extending up to 12 mm. The thicker tantalum-copper coatings (Group 2) were even more effective, with inhibition zones ranging between 13.0 mm to 17.0 mm. Meanwhile, the thicker niobium-copper coatings (Group 2) showed a moderate antifungal effect, generating a delay zone of up to 15.5 mm. In contrast, the thinner niobium-copper coatings (Group 1) showed no antifungal activity. Additionally, the Ti6Al4V titanium alloy after gas-abrasive treatment did not exhibit any inhibitory effect on the growth and proliferation of the bacteria and fungi tested within the observed period. These findings represent the mean values derived from four separate measurement series, maintaining a relative measurement error within 3%.

Consequently, the results indicate that the thicker tantalum-copper coatings (Group 2) were the most effective in inhibiting fungal growth. Additionally, these thicker tantalum-copper coatings, along with the niobium-copper coatings in the same group, demonstrated enhanced antibacterial efficacy. A

similar dependence of antimicrobial properties on the coating thickness was observed by Ilievska *et al.* (5), in which the thicker the MS copper-containing coating, the higher its antimicrobial activity.

Since the MS tantalum-copper coating demonstrated antibacterial and antifungal activity even at a thickness of 2 μm, in contrast to the thin niobium-copper coating, the concentration of released copper ions was assessed for both groups of tantalum-copper coatings on porous scaffolds to analyse the relationship between the number of released ions, bactericidal and antifungal properties and coating thickness. The results of measuring the concentration of Cu<sup>2+</sup> released into a 0.9% sodium chloride solution over 10 days are presented in **Figure 10**.

**Figure 10** illustrates that the coatings' thickness directly impacts the release rate of copper ions into saline solution, which is important for their antibacterial and antifungal efficacy. It is observed that the concentration of released ions decreases in a nonlinear fashion over time, indicating a deceleration in the release process. Notably, despite a significant difference in the initial concentration of ions released by thick and thin coatings approximately twice as much for the former the reduction pattern over time follows a similar trend for both. Specifically, on the first day, the concentration of ions decreases by about 1.3 times for thin coatings and 1.2 times for thick coatings. By the second day, the concentration of ions released is only 1.09 times higher than on the third day for both types of coatings. It can be concluded that the largest number of copper ions is released within the initial 24 h, followed by a decrease in the release rate in the subsequent

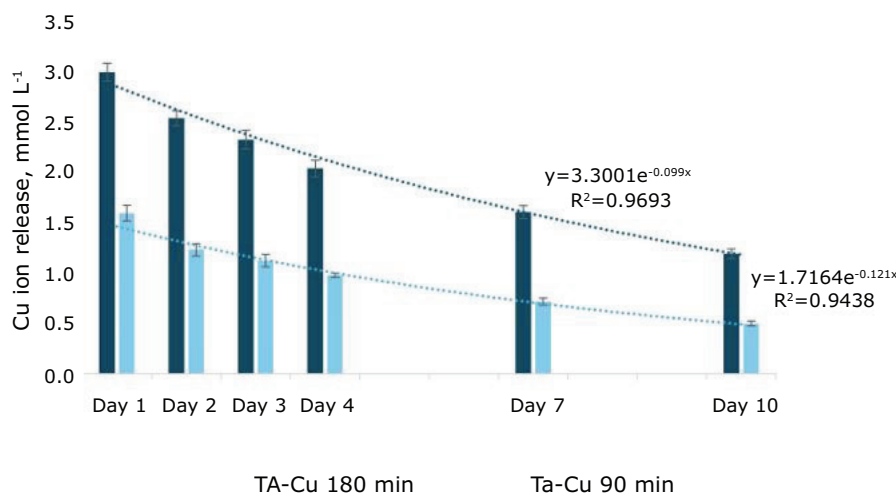


Fig. 10. Release of copper ions into a 0.9% sodium chloride solution within 10 days

days. The curve fitting for copper ion release using a power function (as shown in **Figure 10**) demonstrates a high level of accuracy, with an approximation accuracy of 97% for thicker coatings and 94% for thinner coatings. The degree exponent for the fitting functions are also closely matched. This suggests that the release dynamics of copper ions are primarily dictated by the copper concentration in the coatings rather than by the coating thickness. In comparing the observed time-dependent concentration profiles of copper ion release for these tantalum-copper coatings with data from the release of copper ions from MS titanium-copper films (6–8), we see a slightly different characteristic pattern: rapid release of copper ions within 24 h from titanium-copper film, which is responsible for its cytotoxic effect. That is, for thick coatings (micrometre thickness), there is a monotonic decrease in the curve of the time-dependent concentration profiles of copper ion release and for thin films (nanometre thickness), there is a sharp decrease (6–8). This dynamic release of copper ions is crucial for preventing periprosthetic infections immediately following the implantation of an endoprosthesis. The sustained release profile observed in **Figure 10** suggests a promising approach to effectively prevent infections after surgery since infections can develop up to four weeks post-implantation.

However, the number of copper ions released from tantalum-copper coatings with a micrometre thickness is significantly (almost 5–6 times) higher than the concentrations measured in studies (6–8)) for thin titanium-copper films. On one hand, this could be due to the high surface roughness of the tantalum-copper coated specimens. Zietz *et al.* (8) noted an increase in copper concentration

in the supernatant liquid for rough surfaces due to the increased area in contact with the liquid: compared to a polished surface, a corundum-blasted surface released approximately three times more copper ions within 24 h. On the other hand, it could be due to the thickness of the coatings and the weight percent copper in the coating and may indicate the cytotoxicity of such coatings to osteoblast cells. As previously mentioned in the Introduction section, Ilievska *et al.* (5) demonstrated that the content of copper ions released from copper oxide films, applied for both 5 min and 10 min, was within the safe range for cell viability for the MG-63 cell line, whereas coatings applied for 15 min were cytotoxic to MG-63 cells, as cell viability decreased to about 60%, unlike pure titanium. Apparently, the question of balancing between cytotoxicity properties and the biocompatibility of coatings should be resolved based on *in vitro* testing data, guided by the fact that the release of a large number of copper ions can be harmful to cells and taking into account the ISO 10993-5 standard (9), according to which a reduction in cell viability of more than 30% compared to the control can be considered significantly cytotoxic. Analysing the data presented in **Figure 10**, it can be suggested that there should be an aim to reduce both the thickness of the coatings and, possibly, the weight percent copper in the coating in order to decrease the concentration of released copper ions. This issue requires further study.

**Figure 11** shows specimens of tantalum-copper coatings (Group 2) on porous scaffolds and a control PP disk in a *Candida albicans* nutrient solution at the beginning (**Figure 11(a)**) and at the end of *in vitro* tests (**Figure 11(b)**).

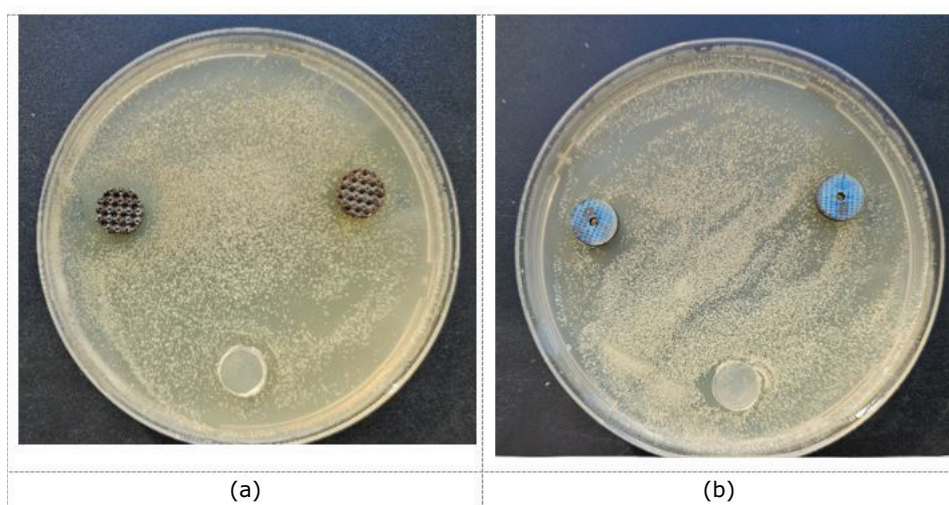


Fig. 11. Tantalum-copper coatings (Group 2) on porous scaffolds and control PP disk in *Candida albicans* nutrient solution: (a) at the beginning of Day 1; (b) at the end of Day 3 of *in vitro* testing

After the third day of *in vitro* testing, visible blue deposits were observed on the coatings, as shown in **Figure 10(b)**. These deposits are presumed to be hexaaqua copper(II) ions  $(\text{Cu}(\text{H}_2\text{O})_6)^{2+}$ , known for their characteristic blue colour, a finding supported by the research of Stranak *et al.* (6). The presence of these blue deposits on all coatings, observed during *in vitro* resistance tests against both fungal and bacterial strains, unequivocally confirms the release of copper ions into the solution. This observation not only demonstrates the coatings' active release of copper but also visually substantiates their potential antimicrobial efficacy.

Comparing the zones of inhibition of *Staphylococcus aureus* bacteria observed in this experiment for MS thick coatings (10  $\mu\text{m}$  thick): up to 24.0 mm for tantalum-copper and up to 25.0 mm for niobium-copper and thin coatings (2  $\mu\text{m}$  thick): up to 20 mm for tantalum-copper and 0 for niobium-copper, as well as the previously observed inhibition zones of up to 17.5 mm for 2%Ti-98%Cu coatings with an average thickness of 5.5  $\mu\text{m}$  on substrates of the Ti6Al4V alloy subjected to gas abrasive treatment (10), we can conclude that the most promising antibacterial MS coating is a thin tantalum-copper coating (Group 1). At the thinnest thickness, 75%Ta-25%Cu coating demonstrates good antibacterial activity, providing zones of inhibition of *Staphylococcus aureus* bacteria of approximately the same order as five times thicker coatings of the same composition or 75%Nb-25%Cu coating, better than 2.5 times thicker 2%Ti-98%Cu coating and better than 75%Nb-25%Cu coating of the same thickness, which does not inhibit bacteria at all.

The results obtained in this study on the antibacterial activity of thick MS tantalum-copper and niobium-copper coatings are generally consistent with the results of Stranak *et al.* (6, 11) and Wojcieszak *et al.* (12, 13), who received thin MS copper-titanium coatings varying from 20 wt% to 80 wt% copper contents demonstrated pronounced antimicrobial activity against *S. aureus*, while remaining relatively non-toxic to the human osteoblast cell line. However, the issue of copper content in dual MS coatings with a thickness in the micrometre range requires further research. We believe that the copper content of thick MS coatings should be reduced to reduce the number of copper ions released and minimise the risk of cytotoxicity to osteoblasts. This can be achieved by reducing the power at the copper target in the magnetron, according to the

paper's results (14), which demonstrated a linear relationship between the power at the target and the content of the target element in the coating. According to our preliminary studies, by reducing the DC on the copper target by 0.5 A, the copper content in the coating can be reduced by two times, while other deposition parameters remain unchanged.

Also, the results of this study confirm the prospects of using tantalum as a second component for the production of antibacterial tantalum-copper MS coatings. Pure tantalum exhibits superior biocompatibility and corrosion resistance properties as a material for MSP coatings on gas-blasted Ti6Al4V alloy, better than CP-Ti (15). At the same time, due to the high specific density and large elastic modulus tantalum, in the production of implants, it is used only in the form of porous scaffolds, which makes it possible to lower the elastic modulus and reduce the weight of the implant (16) and due to its high cost, tantalum is most promising for use as thin coatings. Further research is needed regarding the recommended percentage by weight of copper in the tantalum-copper coating, with analysis of the release of ions from the coating and *in vitro* testing of the antibacterial activity of coatings of different compositions.

## Future Research Perspectives

The research will further examine how the composition (specifically, the weight percent copper) and thickness of tantalum-copper and niobium-copper coatings impact their bactericidal and biocompatibility properties, aiming to elucidate the underlying mechanism of this influence. Additionally, the study will be augmented by analysing the phase composition of the coatings and the effect of phase composition on the release of copper ions in a physiological solution.

Future *in vitro* analyses will be designed to quantify the zone of inhibition for each test day, providing a comprehensive view of antimicrobial activity over time. This will involve measuring the diameter of the zones where bacterial or fungal growth is successfully inhibited, directly indicating the antimicrobial agent's efficacy. Additionally, these measurements will be closely correlated with the concentration of  $\text{Cu}^{2+}$  ions released into the environment.

Further research will also explore the kinetics of copper ion release, investigating how factors such as coating thickness, surface porosity and underlying material composition influence the release profile.

This will include assessing the sustainability of the antimicrobial effect over extended periods, which is crucial for applications in endoprosthesis implants where long-term protection against infection is paramount.

The research strategy encompasses the fabrication of three distinct scaffold types, each characterised by varying levels of porosity, utilising the selective laser melting (SLM) technique. The objective is to systematically assess how these scaffolds' porosity and surface roughness influence the antibacterial efficacy of magnetron-sputtered tantalum-copper and niobium-copper coatings. This evaluation will provide critical insights into optimising the SLM parameters for crafting bactericidal coatings with enhanced performance. By comprehensively analysing the impact of scaffold porosity and surface texture on the antibacterial properties, the study aims to establish specific guidelines for selecting SLM parameters that maximise the antimicrobial effectiveness of MS coatings. Additionally, this investigation will delve into understanding the underlying mechanisms by which these structural characteristics of the scaffolds affect the antibacterial activity, contributing to the development of more effective and reliable surface treatments for medical implants.

The adhesion value of MS coatings will be measured *via* a conventional tensile test. For this purpose, solid cylindrical tensile test specimens will be 3D printed from Ti6Al4V alloy powder with the same SLM parameters that were used in the manufacture of porous scaffolds. It should be noted that usually, the uncoated surface of tensile test specimens is pre-sandblasted to improve the adhesion of glued parts (17, 18); however, this is not planned for 3D printing, since a high surface roughness is expected, higher than that of the Ti6Al4V alloy after gas abrasive treatment (19).

A study of the corrosion resistance of scaffolds with MS coatings in physiological solution, *in vitro* testing of biocompatibility and *in vivo* studies with laboratory animals will be conducted to assess the suitability of MS coatings as both biocompatible and bactericidal coatings for titanium endoprosthesis implants.

## Conclusion

Research demonstrates that utilising dual DC-MS allows for the precise deposition of coatings with specific compositions, namely 75%Ta-25%Cu and 75%Nb-25%Cu, onto porous Ti6Al4V alloy scaffolds. These scaffolds, characterised by a 72%

porosity and a pore diameter of 720  $\mu\text{m}$ , as well as Ti6Al4V alloy surfaces treated with gas abrasion to achieve a Sa of  $4.6 \pm 1 \mu\text{m}$ , effectively receive these targeted coatings. This technique showcases the ability to apply uniform and specified coatings on substrates with varied textures and porosities, highlighting its versatility in preparing surfaces for enhanced biomedical applications.

In this study, MS coatings of 10  $\mu\text{m}$  thickness demonstrated varying degrees of antimicrobial efficacy over three days of testing: tantalum-copper coatings achieved maximum zones of inhibition of 24.0 mm against *Staphylococcus* strains and 17.0 mm against *Candida albicans*, while niobium-copper coatings reached 25.0 mm and 15.5 mm, respectively. Conversely, tantalum-copper coatings at a reduced thickness of 2  $\mu\text{m}$  effectively inhibited bacterial growth up to 20.0 mm and fungal growth to 12.0 mm, whereas niobium-copper coatings of the same thinness and Ti6Al4V alloy substrates showed no inhibitory effect on either bacteria or fungi. These findings highlight three key points: first, thicker tantalum-copper and niobium-copper coatings are more effective at resisting bacterial and fungal infections; second, optimal antimicrobial efficacy of MS coatings on textured surfaces might require thickness in the micrometre range for coating integrity; and third, tantalum-copper coatings are superior for safeguarding endoprosthesis from microbial infections, offering comparable inhibition zones to niobium-copper coatings at one-fifth the thickness.

The time dependence of  $\text{Cu}^{2+}$  ions released into physiological solution from tantalum-copper coatings on porous scaffolds over ten days had a similar monotonically decreasing form for coatings of 10  $\mu\text{m}$  and 2  $\mu\text{m}$  thickness and was characterised by the largest number of ions released in the first 24 h:  $3.07 \pm 0.09 \text{ mmol l}^{-1}$  for thicker and  $1.64 \pm 0.08 \text{ mmol l}^{-1}$  for thinner coatings, showing a direct correlation between coating thickness and their antifungal and antimicrobial efficacy. This release pattern aligns with the growth inhibition zones of both fungal and bacterial strains, highlighting its potential for effectively preventing post-surgical bacterial or fungal infections in endoprosthesis implantation. These findings underscore the potential of integrating 3D printing with MS coating technologies to produce endoprosthesis implants with enhanced surface resistance to both bacteria and fungi. However, further research is needed to find a balance between the biocompatibility and antibacterial activity of the coatings since the number of released copper ions is significant and

indicates the potential cytotoxicity of the coatings to osteoblast cells. This possibility can be mitigated by reducing the copper content and coating thickness.

## Acknowledgments

This research is funded by the Ministry of Science and Higher Education of the Republic of Kazakhstan (AP13268737). The authors express their sincere gratitude to the researcher of the E.O. Paton Electric Welding Institute of NAS of Ukraine, (Kyiv, Ukraine), Voinarovych S for discussing the research results.

## References

1. B. Azamatov, A. Borisov, B. Maratuly, D. Dogadkin, Y. Safarova (Yantsen), R. Yamanoglu, D. Alontseva, *Johnson Matthey Technol. Rev.*, 2025, **69**, (1), 76
2. E. A. Lewallen, W. H. Trousdale, R. Thaler, J. J. Yao, W. Xu, J. M. Denbeigh, A. Nair, J.-P. Kocher, A. Dudakovic, D. J. Berry, R. C. Cohen, M. P. Abdel, D. G. Lewallen, A. J. van Wijnen, *Tissue Eng. Part A*, 2021, **27**, (23–24), 1503
3. B. Jahani, X. Wang, *Biomed. J. Sci. Tech. Res.*, 2021, **38**, (1), 30058
4. E. Avcu, Y. Yildiran Avcu, F. E. Baştan, M. A. U. Rehman, F. Üstel, A. R. Boccaccini, *Prog. Org. Coatings*, 2018, **123**, 362
5. I. Ilievska, V. Ivanova, D. Dechev, N. Ivanov, M. Ormanova, M. P. Nikolova, Y. Handzhiyski, A. Andreeva, S. Valkov, M. D. Apostolova, *Coatings*, 2024, **14**, (4), 455
6. V. Stranak, H. Wulff, P. Ksirova, C. Zietz, S. Drache, M. Cada, Z. Hubicka, R. Bader, M. Tichy, C. A. Helm, R. Hippler, *Thin Solid Films*, 2014, **550**, 389
7. N. Patenge, K. Arndt, T. Eggert, C. Zietz, B. Kreikemeyer, R. Bader, B. Nebe, V. Stranak, R. Hippler, A. Podbielski, *Biofouling*, 2012, **28**, (3), 267
8. C. Zietz, A. Fritsche, B. Finke, V. Stranak, M. Haenle, R. Hippler, W. Mittelmeier, R. Bader, *Bioinorg. Chem. Appl.*, 2012, (1), 850390
9. 'Biological Evaluation of Medical Devices – Part 5: Tests for *in vitro* Cytotoxicity' ANSI/AAMI/ISO 10993-5:2009/(R)2022, American National Standards Institute, Washington, DC, USA, 2009, 49 pp
10. B. N. Azamatov, D. L. Alontseva, A. A. Borisov, B. Maratuly, V. B. Ogay, A. A. Kurmanbaev, *Bull. D. Serikbayev EKTU*, 2022, (3), 40
11. V. Stranak, H. Wulff, H. Rebl, C. Zietz, K. Arndt, R. Bogdanowicz, B. Nebe, R. Bader, A. Podbielski, Z. Hubicka, R. Hippler, *Mater. Sci. Eng.: C*, 2011, **31**, (7), 1512
12. D. Wojcieszak, D. Kaczmarek, A. Antosiak, M. Mazur, Z. Rybak, A. Rusak, M. Osekowska, A. Poniedzialek, A. Gamian, B. Szponar, *Mater. Sci. Eng.: C*, 2015, **56**, 48
13. D. Wojcieszak, M. Osekowska, D. Kaczmarek, B. Szponar, M. Mazur, P. Mazur, A. Obstarczyk, *Coatings*, 2020, **10**, (4), 343
14. A. Bahrami, J. P. Álvarez, O. Depablos-Rivera, R. Mirabal-Rojas, A. Ruíz-Ramírez, S. Muhl, S. E. Rodil, *Adv. Eng. Mater.*, 2017, **20**, (3), 1700687
15. D. Alontseva, Y. Safarova (Yantsen), S. Voinarovych, A. Obrosof, R. Yamanoglu, F. Khoshnaw, H. I. Yavuz, A. Nessipbekova, A. Syzdykova, B. Azamatov, A. Khozhanov, S. Weiß, *Coatings*, 2024, **14**, (2), 206
16. H. Fan, S. Deng, W. Tang, A. Muheremu, X. Wu, P. He, C. Tan, G. Wang, J. Tang, K. Guo, L. Yang, F. Wang, *Biomed Res. Int.*, 2021, (1), 2899043
17. R. Bernardie, R. Berkouch, S. Valette, J. Absi, P. Lefort, *J. Mech. Sci. Technol.*, 2017, **31**, (7), 3241
18. Z. Chen, K. Zhou, X. Lu, Y. C. Lam, *Acta Mech.*, 2014, **225**, (2), 431
19. A. Kadyroldina, D. Alontseva, S. Voinarovych, L. Łatka, O. Kyslytsia, B. Azamatov, A. Khozhanov, N. Prokhorenkova, A. Zhilkashinova, S. Burburska, *Mater. Sci.-Poland*, 2022, **40**, (4), 28

## Authors



Bagdat Azamatov holds a PhD in Automation and Control from D. Serikbayev East-Kazakhstan Technical University (EKTU), where he works as a senior lecturer at the School of Digital Technologies and Artificial Intelligence and as a head of "Smart Engineering" Competence Centre. Currently, Azamatov is doing his postdoctoral research 'Development of Technology for Additive Manufacturing of Patient-Specific Metal Implants with Improved Surface Biocompatibility Properties' (AP13268737) at EKTU under the guidance of Professor Alontseva. His areas of expertise: additive manufacturing, CNC manufacturing of medical implants, surface engineering.



Dmitriy Dogadkin completed a Master of Science in Technical Physics in 2020, then PhD in 2023 from D. Serikbayev EKTU, where he works as a research engineer of “Smart Engineering” Competence Centre. Currently, Dmitriy is writing a PhD thesis and he is a PhD candidate. His areas of expertise: additive manufacturing, CAD/CAE, medical implants, surface engineering, plasma electrolytic oxidation.



Bauyrzhan Maratuly completed his doctoral studies in Mechanical Engineering at D. Serikbayev EKTU and working on his PhD thesis ‘The Effect of Copper Ion Sputtering on the Mechanical and Antibacterial Properties of Titanium Alloy’. Also, he is working as a junior researcher on a project ‘Development of Technology of Bactericidal Coating of Medical Implants Based on Titanium-Copper-Tantalum and Titanium-Copper-Niobium by Magnetron Sputtering Method’ (AP14871715).



Alexander Borisov is a research engineer at the ‘Smart Engineering’ Competence Center at D. Serikbayev EKTU. He graduated sequentially from Bachelor’s, Master’s and postgraduate studies at Novosibirsk State University with a degree in Physics of Ion and Electron Beams and Accelerator Technologies. Scientific interests include nuclear physics and biomedical physics.



Yuliya Safarova (Yantsen) is a senior researcher at the Laboratory of Bioengineering and Regenerative Medicine, National Laboratory Astana. She received PhD degree from the School of Engineering and Digital Sciences, Nazarbayev University, in 2021. Her main areas of research interest are biomedical engineering and stem cells for bone regeneration.



Ridvan Yamanoglu is an academic personnel and researcher at Kocaeli University in Turkey. He is an expert on powder metallurgy, biomedical materials, additive manufacturing and composite materials. So far, Ridvan Yamanoglu has published more than 40 SCI and 50 conference papers. He has recently been working on pressure-assisted sintering and atomisation of metal powders for additive manufacturing.



Darya Alontseva completed her PhD in Physics at East Kazakhstan State University in 2002, then postdoctoral studies in 2013. In 2016 she was awarded the academic title of Professor of Physics. Currently, she is a professor at the School of Digital Technologies and Artificial Intelligence, D. Serikbayev EKTU. Professor Alontseva has 20 years of research experience in developing new materials and processes and leading funded research projects. Her areas of expertise: physics of condensed state and surface engineering. Her current research focuses on the development of robotic technology for MPS of biocompatible coatings onto medical implants.